第 16 卷第 11 期
2026 年 11 月

中国无机分析化学
Chinese Journal of Inorganic Analytical Chemistry

Vol. 16, No. 11
2079～2087

doi: 10. 20236/j. CJIAC. 2026. 11. 011

罗琳杰，汤悦，朱梦姣，等. 多光纤收集系统对锰钢激光诱导等离子体中元素的定性与定量分析[J]. 中国无机分析化学，2026，16(11)：2079-2087.

Luo Linjie, Tang Yue, Zhu Mengjiao, et al. Qualitative and Quantitative Study of Elements in Laser-induced Plasma of Manganese Steel Using a Multi-fiber Collection System[J]. Chinese Journal of Inorganic Analytical Chemistry, 2026, 16(11): 2079-2087.

多光纤收集系统对锰钢激光诱导等离子体中元素的定性与定量分析

罗琳杰　汤 悦　朱梦姣　田 舸　吴昊东　沙开明
张自薪　单悦涵　解宇恒　林庆宇*　段忆翔
（四川大学 机械工程学院，成都 610065）

摘　要　激光诱导击穿光谱(LIBS)技术易因激光诱导等离子体的空间分布不均匀而产生信号波动，传统光谱收集方式难以准确定位等离子体中的最优信号区域，进而影响定量精度。本研究利用多光纤收集LIBS测量系统，对11组不同锰钢样品的激光诱导等离子体进行二维分布表征，分析Mn(Ⅰ)601. 66 nm、Mn(Ⅱ)612. 24 nm、Cr(Ⅰ)520. 92 nm和Fe(Ⅰ)523. 07 nm等元素分布图像，验证了等离子体中存在的元素分布不均匀性，并定位了适用于定量分析的光强峰值区域。针对各样品等离子体的特征区域进行Mn、Cr 和Fe的定量分析方法研究。定量结果表明，四种特征谱线的定量线性相关系数(R^2)分别为0. 997 5、0. 925 8、0. 916 1和0. 851 0，均表现出较为良好的相关性，结合相对标准偏差(RSD)和相对误差(RE)综合分析，证实了该多光纤收集LIBS系统具备多元素同时定量分析的能力。该多光纤收集系统可提升LIBS的定量分析性能。

关键词　激光诱导击穿光谱(LIBS)；等离子体；元素空间分布；多元素定量分析；锰钢

要点

1）利用多光纤LIBS系统，实现激光等离子体中元素的二维空间分布表征。

2）研究了锰钢激光等离子体中元素分布的不均匀性及谱线强度的空间聚集性。

3）基于多光纤收集系统的定标曲线显示了高度线性相关性。

中图分类号：O657. 38　　**文献标志码**：A　　**文章编号**：2095-1035(2026)11-2079-09

激光诱导击穿光谱(LIBS)技术是一种基于高能激光脉冲与物质相互作用产生等离子体，并通过分析等离子体中原子或离子发射光谱实现元素成分和含量快速分析的光谱分析技术[1-4]。该技术凭借其无需复杂样品预处理[5-6]、可实现多元素同时检测[7-8]、分析速度快[9-10]、可适应恶劣环境[11-12]等突出优势，近年来受到学术界和工业界的广泛关注。目前LIBS技术已被成功应用于众多领域，如煤炭品质分析[13-14]、地球科学[15-16]、生物科学[17-18]、工业冶金[19-20]以及金属材料分析[21-22]等。特别是在钢铁冶金行业，LIBS技术展现出巨大的应用潜力[23]。

收稿日期：2025-11-02　**修回日期**：2026-01-07　**录用日期**：2026-01-09　**在线出版日期**：2026-06-17
Received：2025-11-02　**Revised**：2026-01-07　**Accepted**：2026-01-09　**Online published**：2026-06-17
基金项目：国家自然科学基金资助项目(62475174)
Fund：Supported by the National Natural Science Foundation of China (62475174)

作者简介：罗琳杰，男，硕士研究生，主要从事激光光谱定量方法研究。E-mail：1321996779@qq. com
Author：Luo Linjie, male, master′s candidate, mainly engaged in research on quantitative methods of laser spectroscopy. E-mail：1321996779@qq. com
*通信作者：林庆宇，男，副研究员，主要从事激光光谱分析仪器研发。E-mail：qylin@scu. edu. cn
*Corresponding author：Lin Qingyu, male, associate researcher, mainly engaged in the development of laser spectroscopy instruments. E-mail：qylin@scu. edu. cn

©Chinese Journal of Inorganic Analytical Chemistry Editorial Department 2026. This is an open access article under the CC-BY-NC-ND 4. 0 License.

相比而言，传统分析方法依赖于人工取样和实验室离线检测，存在时效滞后。而LIBS技术可在数秒内完成对钢铁中多元素(如C、Si、Mn、P及S等)的在线定量分析，实现连续在线监测。早在20世纪80年代末，日本相关企业已尝试将LIBS技术引入钢液成分的在线监测中，显著减少了传统取样分析带来的时间延迟[24]。此后，国内外学者围绕LIBS在钢铁分析中的定量方法开展了大量研究。Ren等[25]开发了结合LIBS技术与序贯后向选择-随机森林(SBS-RF)算法的定量分析方法，对合金钢中有害元素P和S进行检测，SBS-RF模型对S(R^2=0.9991)和P(R^2=0.9994)的预测效果优于单变量方法、PLS模型和传统RF模型。Yang等[26]提出了一种基于迁移学习的高温合金钢LIBS定量分析方法，解决了高温环境下校准模型的适应性问题，实现了高温条件下合金钢中多种元素的准确快速定量分析。Peterson等[27]测试评估了一套用于钢渣快速分析的LIBS系统，首次探索了通过脉冲分布分析(PDA)技术区分金属铁与氧化铁含量的可能性，结果显示LIBS有望成为实现该目标的快速准确技术。Silva等[28]测试了手持LIBS仪器对46个高炉生铁样品中C、Mn、P、Si、Ti的定量分析性能，通过PLS多元校正模型实现了比单变量方法更优的准确性，为冶金现场快速成分检测提供了可行方案。Chen等[29]利用长短双脉冲LIBS技术，尝试解决钢铁样品表面碳污染的干扰问题，实现了对低含量碳(100 μg/g)的精确测量。杨淋玉等[30]采用遗传算法结合偏最小二乘方法对钢铁样品中的Mn和Ni进行定量分析，有效提高了模型的预测精度。郑培超等[31]提出了一种基于等离子体图像的光谱信号筛选方法，通过优化信号选择策略，显著改善了定标模型性能。童巨红等[32]构建了一种自吸收效应量化模型，在校正自吸收效应后提升了LIBS定量分析精度。Quackatz等[33]将无标样LIBS(CF-LIBS)技术应用于双相不锈钢GTAW焊接过程中的原位化学成分分析，与PLS分析结果对比验证了其准确性，为焊接过程中金属元素分布与焊缝缺陷关联性研究提供了新方法。

然而，尽管LIBS技术在钢铁行业中取得了一定进展，其定量分析的精度仍面临挑战。主要问题之一是源于激光诱导等离子体复杂的时空演化特性：激光诱导等离子体在形成和膨胀过程中，其温度、电子密度及元素分布存在显著的空间不均匀性，导致不同空间位置采集的光谱信号强度波动较大，影响分析的重复性和准确性[34]。当前，LIBS装置中多采用单点探头或固定位置的光纤收集系统，但这种收集方式忽略了激光诱导等离子体中元素的空间分布差异，导致定量精度受到了影响。针对该问题，本研究旨在：1)利用多光纤收集LIBS系统定位锰钢等离子体中不同目标元素的强度聚集区域；2)针对该强度聚集区域，采用线性模型对目标元素进行定量分析，再由结果验证本多光纤收集LIBS系统的定量性能，为钢铁多元素LIBS定量分析提供空间优化新方式。

1 实验部分

1.1 锰钢样本

为验证本系统的定性及定量分析性能，本研究选用11种锰钢标样进行测试，锰钢样品中目标元素的含量存在不同梯度，适用于不同含量元素的定量分析研究，所有样品在测试前均已进行表面清理。表1展示了各锰钢样品编号及目标元素的对应含量。

表1 锰钢标样编号及Fe、Mn、Cr含量

Table 1 Sample numbers and Fe, Mn, Cr contents of manganese steel samples /%

Samples	Fe	Mn	Cr
TS T022-5	68.40	26.23	1.73
TS T022-6	66.16	30.54	0.20
ZGMn7	82.07	7.23	3.01
ZGMn10Cr2	83.64	9.84	1.56
ZGMn13Cr2-A	77.17	13.97	1.91
ZGMn13Cr2-B	84.79	11.82	1.51
ZGMn18Cr2-A	77.13	16.90	2.20
ZGMn18Cr2-B	76.31	18.70	2.00
ZGMn20	75.14	20.99	0.05
ZGMn22Cr2	71.43	22.39	1.23
ZGMn24Cr2	69.47	24.20	1.86

1.2 LIBS系统及参数设置

多光纤收集LIBS测量系统整体结构如图1所示。激光器采用Nd:YAG型激光器(波长1 064 nm)，设定重复频率为5 Hz，单次脉冲能量为100 mJ。设置光谱仪的采集曝光时间为5 s，在每次连续曝光过程中，探测器实际记录的是该时间段内所有脉冲激发的等离子体光谱信号的积分强度。光纤阵列内腔集成100根数值孔径0.22且纤芯直径400 μm的

石英光纤，形成面阵输入端(10×10矩形排列，面积8 mm×8 mm)和线阵输出端(1×100直线排列，长度75 mm)。所有光纤均用标准光源进行响应校正以消除光强传输效率差异。光谱探测范围400～700 nm，通过汞灯的Hg(Ⅰ)546.08 nm 谱线半峰宽表征系统分辨率为1.2 nm。

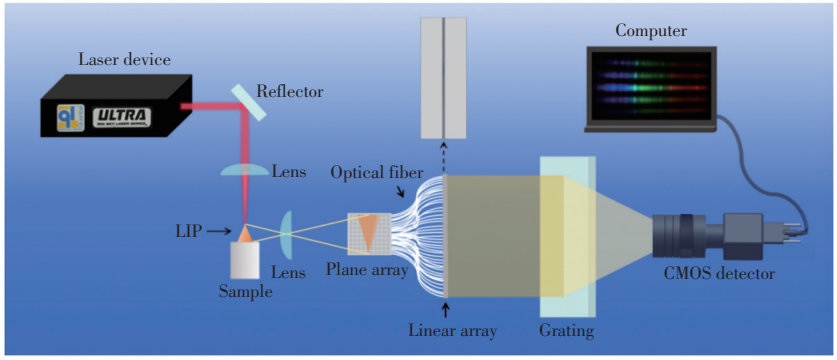


图1　多光纤收集LIBS测量系统

Figure 1　Multi-fiber LIBS measurement system.

1.3　图像采集及预处理

针对锰钢样品，在表面随机选取15个不同位置进行光谱采集，最终用于元素定量分析的数据为每次采集所得的光谱信号总和的平均值。采用二维中值滤波函数对原始图像进行去噪预处理后将图像转换为灰度图[35]。进行等离子体的二维光强分布表征时在每个通道采集42个像素点的平均灰度值，在进行归一化处理后，乘以对应通道的强度响应校正系数，从而得到100个通道的最终灰度值，以此表征每个通道的光谱强度；元素定量分析时，读取目标光谱线上2 448个像素点的灰度值，以像素点横坐标对应波长值，每个像素点所对应的灰度值作为强度值，由此构建单通道光谱响应曲线。

2　结果与讨论

2.1　多元素定性分析

采用多光纤收集LIBS系统，测量了各锰钢样品的光谱曲线。结果表明，各样品在400～700 nm波长区域内存在显著的特征谱线(图2a、2b)，但各样本相同元素的光谱曲线在整体强度及轮廓上呈现出一定差异，选取差别较大的三个样品的光谱曲线进行对比(图2b)。由于Cr(Ⅰ)520.92 nm、Fe(Ⅰ)523.07 nm、Mn(Ⅰ)601.66 nm和Mn(Ⅱ)612.24 nm等元素的特征谱线强度较强，且无临近干扰，信噪比较好，选取这四个元素特征峰进行分析，图2c－2f标注了各元素特征峰的谱线位置。由图2可知，各样品的对应元素特征峰轮廓一致且峰形尖锐，但信号强度存在明显差异。特征谱线强度与样品中相应元素的含量呈正相关，其中锰元素的相关性尤为显著。上述结果验证了所搭建的多光纤收集LIBS系统具备基本的元素探测能力。

2.2　多元素二维表征

利用多光纤收集系统对等离子体中的Mn(Ⅰ)601.66 nm、Mn(Ⅱ)612.24 nm、Cr(Ⅰ)520.92 nm和Fe(Ⅰ)523.07 nm特征谱线进行分辨率为10×10的二维强度分布，结果如图3所示。分析可得，各元素光强在等离子体中呈现出非均匀分布，且在所有图中，光强峰值稳定位于等离子体中心区域，其他区域的光强随着与峰值区域之间的距离增加而逐渐递减。本研究选择该光强峰值区域内所得光谱进行后续定量分析研究。

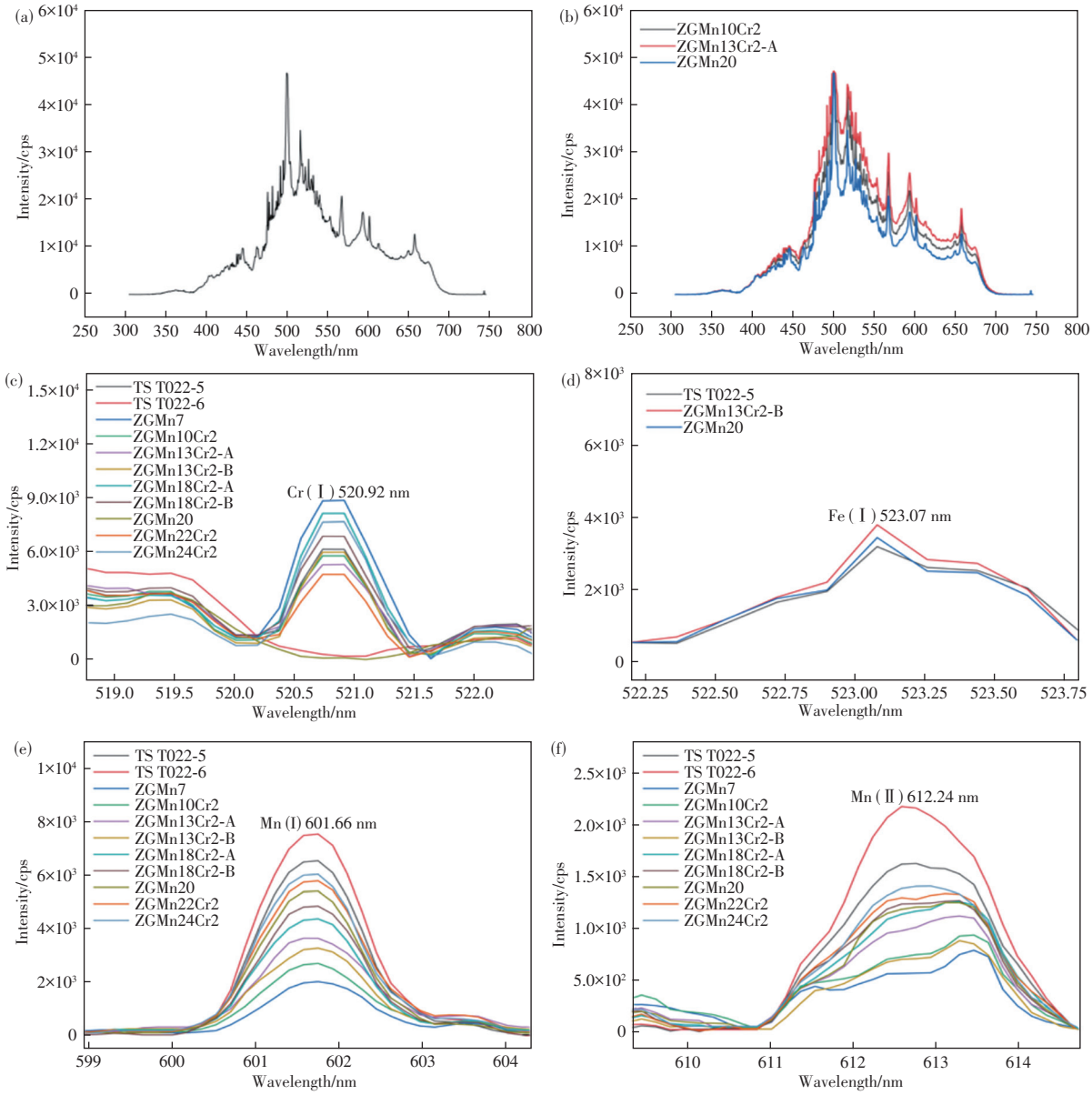


图2 系统光谱图：(a)ZGMn20样品光谱图；(b)3种锰钢样品光谱图；(c)–(f)11种锰钢样品Cr(Ⅰ)520.92 nm、Fe(Ⅰ)523.07 nm、Mn(Ⅰ)601.66 nm和Mn(Ⅱ)612.24 nm的光谱图

Figure 2 System spectrogram: (a) Spectrogram of ZGMn20 sample; (b) Spectrogram of 3 manganese steel samples; (c)–(f) Spectrograms of Cr(Ⅰ)520.92 nm, Fe(Ⅰ)523.07 nm, Mn(Ⅰ)601.66 nm and Mn(Ⅱ)612.24 nm for the 11 manganese steel samples.

2.3 多元素定量分析

随机选择ZGMn10Cr2和ZGMn18Cr2-B样品的数据作为验证集，剩余9个标样的采集数据用于建立标准曲线。标准曲线结果如图4所示。从图4中可看出Mn(Ⅰ)601.66 nm、Mn(Ⅱ)612.24 nm、Cr(Ⅰ)520.92 nm和Fe(Ⅰ)523.07 nm的线性拟合效果良好。其中，Mn(Ⅰ)601.66 nm的相关系数(R^2)为0.997 5，表明所搭建的多光纤收集LIBS系统对Mn的线性曲线可靠性很高；Mn(Ⅱ)612.24 nm和Cr(Ⅰ)520.92 nm的R^2分别为0.925 8和0.916 1，表明其定量可靠性较强；Fe(Ⅰ)523.07 nm的R^2值较低，为0.851 0，分析认为主要因为Fe作为基体元素，在各样品中含量最大，其浓度梯度变化范围相对较小，在这种小动态范围内，仪器噪声、等离子体波动以及基体效应引起的微小偏差会对拟合残差产生更为显著的贡献，从而降低R^2值；其次，该谱线强度较高，易受探测器饱和效应干扰[36]，最终导致校准曲线R^2较低。后续优化手段可尝试采用背景扣除算法

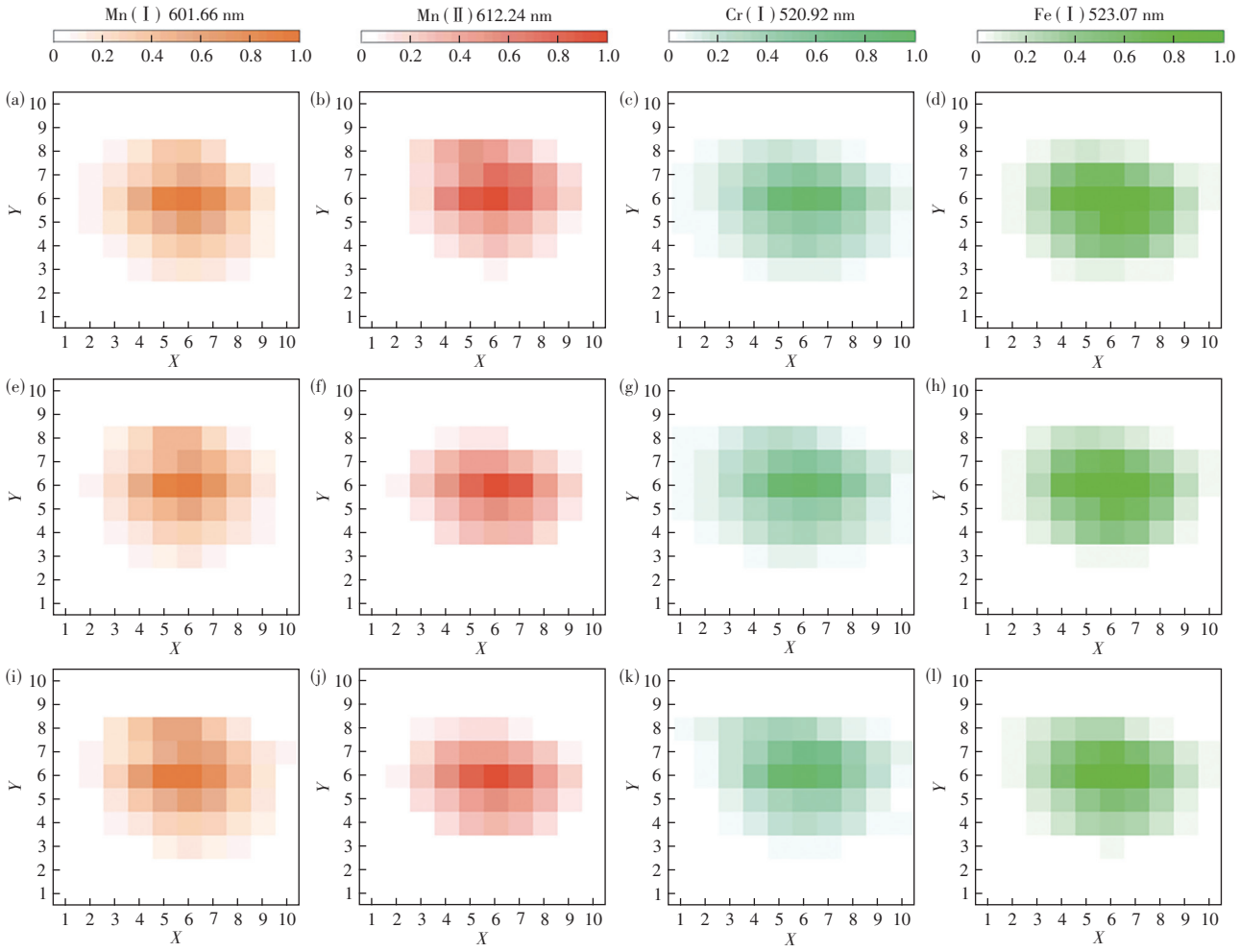


图3　Mn(Ⅰ)601.66 nm、Mn(Ⅱ)612.24 nm、Cr(Ⅰ)520.92 nm和Fe(Ⅰ)523.07 nm目标元素二维分布表征图：(a)-(d) TS T022-5样品；(e)-(h) ZGMn10Cr2样品；(i)-(l) ZGMn20样品

Figure 3　2D distribution mapping of target elements Mn(Ⅰ)601.66 nm, Mn(Ⅱ)612.24 nm, Cr(Ⅰ)520.92 nm and Fe(Ⅰ)523.07 nm: (a)-(d) TS T022-5 sample; (e)-(h) ZGMn10Cr2 sample; (i)-(l) ZGMn20 sample.

或选择次要谱线减少饱和效应。

采用标准样品的相对标准偏差作为评价系统定量结果的指标，如式(1)所示。

$$\mathrm{RSD}=\frac{1}{\bar{x}}\sqrt{\frac{\sum\left(x_m-\bar{x}\right)^2}{n-1}}\times 100\% \tag{1}$$

其中 x_m 为某样品第 m 次采集数据的强度值，$\bar{x}$ 为该样品所有采集次数数据总和的平均强度值，n 为采集总次数。

由表2数据可知，Mn(Ⅰ)601.66 nm、Mn(Ⅱ)612.24 nm、Cr(Ⅰ)520.92 nm和Fe(Ⅰ)523.07 nm四种元素特征波段的平均相对标准偏差(RSD)分别为12.43%、21.35%、21.02%和16.84%。值得注意的是，ZGMn7样品中Mn(Ⅱ)612.24 nm的RSD为43.36%，TS T022-6与ZGMn20样品中Cr(Ⅰ)520.92 nm的RSD分别达到56.30%和44.76%，这一异常波动与元素的低含量有关，低含量会导致LIBS光谱信号强度减弱，并更易受基体效应或元素间干扰的影响，从而使测量结果的标准偏差增大。

采用验证样品的真实值和预测值的相对误差作为评价系统定量结果的指标，见式(2)。

$$\mathrm{RE}=\left|\frac{(x_i-\hat{x}_i)}{x_i}\right|\times 100\% \tag{2}$$

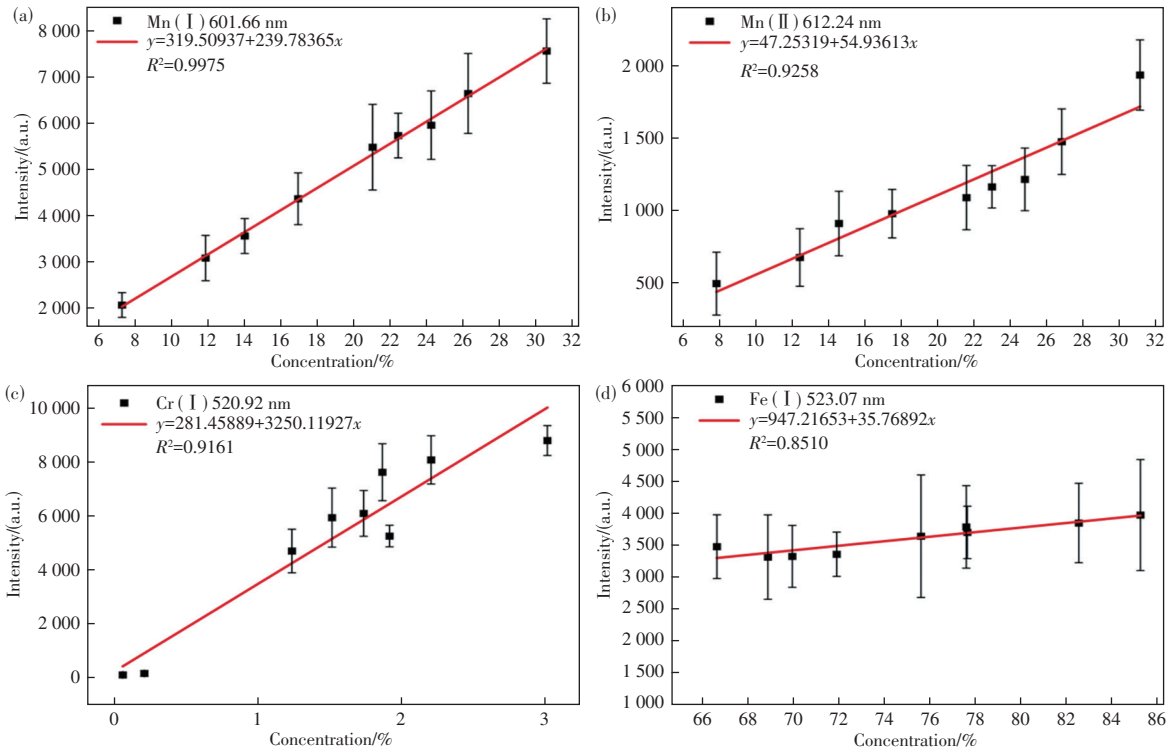


图4 元素定量标准曲线

Figure 4 Calibration curve for elemental quantification.

表2 各标准样品目标元素相对标准偏差

Table 2 Relative deviation results of target elements in each standard sample relative standard deviation(RSD) /%

Samples	Mn(Ⅰ)	Mn(Ⅱ)	Cr(Ⅰ)	Fe(Ⅰ)
TS T022-5	12.98	15.29	13.86	19.92
TS T022-6	9.19	12.51	56.30	14.34
ZGMn7	12.84	43.36	6.27	16.14
ZGMn13Cr2-A	10.56	24.32	7.60	11.08
ZGMn13Cr2-B	15.82	29.16	18.35	21.86
ZGMn18Cr2-A	12.77	17.03	11.07	17.05
ZGMn20	16.87	20.30	44.76	26.31
ZGMn22Cr2	8.40	12.51	17.10	10.30
ZGMn24Cr2	12.40	17.71	13.84	14.56
Mean values	12.43	21.35	21.02	16.84

式中，x_i为验证样品i中目标元素的真实值(%)；$\hat{x}_i$是验证集样品i中目标元素的预测值(%)。

通过两个验证样品中4种目标发射谱线的预测含量与实际标准值相比较，可以看出，ZGMn10Cr2样品中Mn(Ⅰ)601.66 nm、Mn(Ⅱ)612.24 nm、Cr(Ⅰ)520.92 nm和Fe(Ⅰ)523.07 nm等预测含量的相对误差分别为0.71%、1.83%、8.33%和0.35%；ZGMn18Cr2-B样品中Mn(Ⅰ)601.66 nm、Mn(Ⅱ)612.24 nm、Cr(Ⅰ)520.92 nm和Fe(Ⅰ)523.07 nm等预测含量的相对误差分别为1.82%、4.12%、1.00%和2.04%。表明所搭建的多光纤收集LIBS系统具有良好的定量预测能力。然而，系统对ZGMn10Cr2样本中的Cr(Ⅰ)的定量相对误差为8.33%，分析这主要是源于该元素谱线干扰所导致的线性模型对该基体成分的预测差异。结果如表3所示。

表3 预测值及相对误差(RE)结果

Table 3 Predicted values and relative error(RE) results /%

Elements	ZGMn10Cr2			ZGMn18Cr2-B		
	Standard content	Predicted content	Relative error	Standard content	Predicted content	Relative error
Mn(Ⅰ)	9.84	9.91	0.68	18.70	19.04	1.82
Mn(Ⅱ)	9.84	10.02	1.83	18.70	19.47	4.12
Cr(Ⅰ)	1.56	1.69	8.33	2.00	2.02	1.00
Fe(Ⅰ)	83.64	83.35	0.35	76.31	77.87	2.04

基于上述结果得出：在实现对等离子体中元素二维分布表征的基础上，该多光纤收集LIBS系统具备对元素进行定量检测的能力。其中，对Mn(Ⅰ)601.66 nm的线性模型可靠且精度优异，而对Cr(Ⅰ)520.92 nm和Mn(Ⅱ)612.24 nm的定量模型虽拟合效果较好但相对误差大，后续需进一步优化研究，Fe(Ⅰ)523.07 nm的模型则线性关系相对最弱且离散性较为显著，需调整实验参数或增加重复测量以提高精度。

3　结论

本研究通过多光纤收集LIBS系统实现了激光等离子体中元素空间分布强度的二维表征，验证了锰钢激光等离子体中元素分布的不均匀性及空间聚集效应。针对元素强度峰值区域进行了多元素定量分析，结果中目标元素的定标曲线均显示出较高的线性相关性，初步证明了系统在多元素定量分析中的可行性。研究结果证明激光诱导等离子体中元素分布的空间规律与系统定量性能存在内在关联，优化信号采集位置能辅助解决传统LIBS技术信号稳定性差的问题，为LIBS技术的精度提升提供新方法支撑。

参考文献

[1] Alashmawy A. Laser-induced breakdown spectroscopy: basic fundamentals, principle, measuring parameters and applications[J]. Journal of Basic and Environmental Sciences, 2023, 10(1): 39-48.

[2] Hou Guanyu, Wang Ping, Tong Cunzhu. Progress in laser-induced breakdown spectroscopy and its applications[J]. Chinese Optics, 2013, 6(4): 490-500.

[3] 闫文豪，杨晓莹，耿鑫，等. 手持式LIBS结合随机森林用于鱼产品的快速鉴别分析[J]. 光谱学与光谱分析，2022，42(12)：3714-3718.
Yan Wenhao, Yang Xiaoying, Geng Xin, et al. Identification of fish products using handheld laser induced breakdown spectroscopy combined with random forest[J]. Spectroscopy and Spectral Analysis, 2022, 42(12): 3714-3718.

[4] 杨友良，王禄，马翠红. LIBS检测钢液Mn元素的实验条件优化[J]. 激光杂志，2020，41(2)：29-32.
Yang Youliang, Wang Lu, Ma Cuihong. Optimization of experimental conditions for detecting Mn element in molten steel by LIBS detection[J]. Laser Journal, 2020, 41(2): 29-32.

[5] Vikas G, Kumar A R, Tejmani K, et al. Compositional analysis of copper and iron-based alloys using LIBS coupled with chemometric method[J]. Analytical Sciences, 2023, 40(1): 53-65.

[6] Zhang Siyu, Huang Zhenlin, Zhao Zhifang, et al. Quantitative analysis of mineral elements in hair and nails using calibration-free laser-induced breakdown spectroscopy[J]. Optik, 2021, 242: 167067. DOI: 10.1016/j.ijleo.2021.167067.

[7] Martins S B, Noronha Gustavo, Silva S G, et al. Multi-elemental analysis of landfill leachates by single and double pulse laser-induced breakdown spectroscopy[J]. Microchemical Journal, 2021, 165: 106125. DOI: 10.1016/j.micro.2021.106125.

[8] Ma Qiang, Liu Zhong, Zhang Tao, et al. Multielement simultaneous quantitative analysis of trace elements in stainless steel via full spectrum laser-induced breakdown spectroscopy[J]. Talanta, 2024, 272: 125745. DOI: 10.1016/j.talanta.2024.125745.

[9] Harmon S R, Wise A M, Curry C A, et al. Rapid analysis of muscovites on a lithium pegmatite prospect by handheld LIBS[J]. Minerals, 2023, 13(5): 697. DOI: 10.3390/min 13050697.

[10] Li Jingjun, Yao Jiangfei, Han Yutao, et al. A study of the temperature variation effect in a steel sample for rapid analysis using LIBS[J]. Optics and Laser Technology, 2022, 147: 107707. DOI: 10.1016/j.optlastec.2022.107707.

[11] Almaviva S, Karino T, Akaoka K, et al. LIBS as diagnostics of analytical chemistry for surface mapping of complex mixed samples simulating debris inside the TEPCO's Fukushima Daiichi Nuclear Power Plant (FDNPS) reactor cores[J]. Spectrochimica Acta Part B: Atomic Spectroscopy, 2024, 218: 106960. DOI: 10.1016/j.sab.2024.106960.

[12] Luo Yong, Chen Zhe, Liu Jun, et al. Quantification and geological implications of manganese, barium, and copper observed by MarSCoDe LIBS at Zhurong landing site on Mars[J]. Icarus, 2026, 443: 116781. DOI: 10.1016/j.icarus.2026.116781.

[13] Niu Xin, Guan Feng, Li Zhe, et al. A temporal and spatial dual-dimension fusion spectra mapping method for rapid detection of coal quality in laser-induced breakdown spectroscopy[J]. Talanta, 2025, 293: 128106. DOI: 10.1016/j.talanta.2025.128106.

[14] Zhang Lei, Gong Yan, Li Yue, et al. Development of a coal quality analyzer for application to power plants based on laser-induced breakdown spectroscopy[J]. Spectrochimica Acta Part B: Atomic Spectroscopy, 2015, 113: 167-173.

[15] Devangad P, Unnikrishnan V K, Nayak R, et al. Performance evaluation of laser induced breakdown spectroscopy (LIBS) for quantitative analysis of rare earth elements in phosphate glasses[J]. Optical Materials, 2016, 52: 32-37.

[16] Alvarez-Llamas C, Purohit P, Moros J, et al. LIBS acoustic mid-level fusion scheme for mineral differentiation under terrestrial and martian atmospheric conditions[J]. Analytical Chemistry, 2022, 94(3): 1840-1849.

[17] Wan Xin, Wang Peng. Analysis of heavy metals in organisms based on an optimized quantitative LIBS[J]. Optik, 2015, 126(19): 1930-1934.

[18] Khan M N, Wang Qianqian, Idrees B S, et al. A review on laser-induced breakdown spectroscopy in different

cancers diagnosis and classification[J]. Frontiers in Physics, 2022, 10: 821057. DOI: 10.3389/fphy.2022.821057.

[19] 任祥旭, 孔令华, 郑积仕, 等. 基于卡尔曼滤波与机器学习的激光诱导击穿光谱钢铁多元素定量分析探究[J]. 冶金分析, 2023, 43(6): 19-29.
Ren Xiangxu, Kong Linghua, Zheng Jishi, et al. Quantitative analysis of multiple elements in steel by laser-induced breakdown spectroscopy based on Kalman filter and machine learning[J]. Metallurgical Analysis, 2023, 43(6): 19-29.

[20] Gudmundsson H S, Matthiasson J, Björnsson M B, et al. Quantitative in-situ analysis of impurity elements in primary aluminum processing using laser-induced breakdown spectroscopy[J]. Spectrochimica Acta Part B: Atomic Spectroscopy, 2019, 158: 105646. DOI: 10.1016/j.sab.2019.105646.

[21] Syed D U Z, Shen Chenglin, Zhao Qinduan, et al. Evaluation of the laser cleaning efficacy of Q235 steel using laser-induced breakdown spectroscopy[J]. Metals, 2022, 13(1): 59. DOI: 10.3390/met.13010059.

[22] Ran Hong, Tian Weina, Ding Wei, et al. Quantitative analysis of titanium alloys using one-point calibration laser-induced breakdown spectroscopy[J]. Applied Physics B, 2021, 127(3): 54. DOI: 10.1007/s00340-021-07581-4.

[23] Li Shu, Qin Zhi, Lu Yang, et al. High-throughput microanalysis of steel segregation using picosecond laser-induced breakdown spectroscopy[J]. Talanta, 2025, 295: 128229. DOI: 10.1016/j.talanta.2025.128229.

[24] 吴少波, 张云贵, 于立业, 等. 基于LIBS的熔态金属成分在线分析技术的现状及发展趋势[J]. 冶金自动化, 2013, 37(3): 1-6.
Wu Shaobo, Zhang Yungui, Yu Liye, et al. State-of-art and trend of molten metal online analysis based on Laser-Induced Breakdown Spectroscopy[J]. Metallurgical Industry Automation, 2013, 37(3): 1-6.

[25] Ren Fangqi, Qin Juan, Yang Chunhua, et al. Quantitative detection of harmful elements in alloy steel by LIBS technique and sequential backward selection-random forest (SBS-RF)[J]. Journal of Analytical Atomic Spectrometry, 2017, 32(11): 2194-2199.

[26] Yang Jianhong, Liu Xiaomeng, Li Huili, et al. An LIBS quantitative analysis method for alloy steel at high temperature based on transfer learning[J]. Journal of Analytical Atomic Spectrometry, 2018, 33(7): 1184-1195.

[27] Peterson J, Gatty G M, Bengtson A. Rapid chemical analysis of steel slag by laser-induced breakdown spectroscopy for near-the-line applications[J]. Journal of Analytical Atomic Spectrometry, 2020, 35(9): 1848-1858.

[28] Silva S G, Dall′Olio Olga, Bortoli Aldo, et al. Quantitative analysis of pig iron from steel industry by handheld laser-induced breakdown spectroscopy and partial least square (PLS) algorithm[J]. Applied Sciences, 2020, 10(23): 8461. DOI: 10.3390/app10238461.

[29] Chen Minchao, Gao Haorong, Chen Yada, et al. Quantitative analysis of trace carbon in steel samples using collinear long-short double-pulse laser-induced breakdown spectroscopy[J]. Spectrochimica Acta Part B: Atomic Spectroscopy, 2022: 106398. DOI: 10.1016/j.sab.2022.106398.

[30] 杨淋玉, 丁宇, 战晔, 等. 基于LIBS与GA-PLS的钢铁中Mn, Ni元素定量分析研究[J]. 光谱学与光谱分析, 2022, 42(6): 1804-1808.
Yang Linyu, Ding Yu, Zhan Ye, et al. Quantitative analysis of Mn and Ni in steel based on LIBS combined with GA-PLS algorithm[J]. Spectroscopy and Spectral Analysis, 2022, 42(6): 1804-1808.

[31] 郑培超, 刘少剑, 王金梅, 等. LIBS结合图像筛选方法提高钢铁中Cu、Cr、Mn检测稳定性研究[J]. 中国无机分析化学, 2024, 14(2): 223-232.
Zheng Peichao, Liu Shaojian, Wang Jinmei, et al. Study on improving detection stability of Cu, Cr and Mn in steel by LIBS combined with image screening method[J]. Chinese Journal of Inorganic Analytical Chemistry, 2024, 14(2): 223-232.

[32] 童巨红, 袁梦甜, 王朋, 等. 基于激光诱导击穿光谱对钛元素自吸收效应的分析[J]. 中国无机分析化学, 2024, 14(2): 233-238.
Tong Juhong, Yuan Mengtian, Wang Peng, et al. Analysis of self-absorption effect of titanium based on laser-induced breakdown spectroscopy[J]. Chinese Journal of Inorganic Analytical Chemistry, 2024, 14(2): 233-238.

[33] Quackatz L, Gornushkin I, Griesche A, et al. In situ chemical analysis of duplex stainless steel weld by laser induced breakdown spectroscopy[J]. Spectrochimica Acta Part B: Atomic Spectroscopy, 2024, 214: 106899. DOI: 10.1016/j.sab 2024.106899.

[34] D′Angelo A C, Pace D M D, Bertuccelli G, et al. Laser induced breakdown spectroscopy on metallic alloys: solving inhomogeneous optically thick plasmas[J]. Spectrochimica Acta Part B: Atomic Spectroscopy, 2007, 63(3): 367-374.

[35] 刘嘉敏, 彭玲, 袁佳成, 等. 基于二维变分模态分解和自适应中值滤波的图像去噪方法[J]. 计算机应用研究, 2017, 34(10): 3149-3152.
Liu Jiamin, Peng Ling, Yuan Jiacheng, et al. Image denoising method based on bi-dimensional variational mode decomposition and adaptive median filtering[J]. Application Research of Computers, 2017, 34(10): 3149-3152.

[36] 钟奇秀, 赵天卓, 李欣, 等. 多元素LIBS分析的标准化交叉验证及其优化[J]. 光谱学与光谱分析, 2020, 40(2): 622-627.
Zhong Qixiu, Zhao Tianzhuo, Li Xin, et al. Standardized cross-validation and its optimization for multi-element LIBS analysis[J]. Spectroscopy and Spectral Analysis, 2020, 40(2): 622-627.

Qualitative and Quantitative Study of Elements in Laser-induced Plasma of Manganese Steel Using a Multi-fiber Collection System

Luo Linjie, Tang Yue, Zhu Mengjiao, Tian Ze, Wu Haodong, Sha Kaiming, Zhang Zixin, Shan Yuehan, Xie Yuheng, Lin Qingyu*, Duan Yixiang

(*School of Mechanical Engineering, Sichuan University, Chengdu, Sichuan 610065, China*)

Abstract Laser-induced breakdown spectroscopy (LIBS) often suffers from significant spectral signal fluctuations during practical applications due to the spatial inhomogeneity of plasma in its temporal evolution, which adversely affects the accuracy and stability of quantitative analysis. The traditional single-point acquisition mode struggles to capture the region of strongest plasma radiation, limiting the further application of LIBS technology in elemental quantitative analysis. To overcome this limitation, this study designed a LIBS measurement system based on a multi-fiber planar array acquisition method. One end of 100 multimode optical fibers was arranged in a 10×10 rectangular array to achieve two-dimensional spatially resolved collection of laser-induced plasma radiation. Each fiber independently collects emission signals from corresponding sub-regions of the plasma. After transmission through the fibers, the signals are rearranged at the other end into a 1×100 linear array output, thereby achieving two-dimensional spatial segmentation and synchronous measurement of plasma radiation. Experiments selected 11 manganese steel samples with known compositions. Using the constructed system, two-dimensional intensity distribution imaging was performed for characteristic spectral lines, including Mn (Ⅰ) 601.66 nm, Mn (Ⅱ) 612.24 nm, Cr (Ⅰ) 520.92 nm, and Fe (Ⅰ) 523.07 nm. The results revealed significant differences in the spatial distribution of radiation intensity for different elements within the plasma, demonstrating notable inhomogeneity and spatial aggregation characteristics. Based on this two-dimensional distribution information, the peak radiation regions of each element were accurately located, providing optimal signal acquisition positions for subsequent quantitative analysis. Based on this, quantitative analysis of multiple elements (Mn, Cr, Fe) was conducted for the characteristic regions of the plasma in each sample. The quantitative calibration results showed that the coefficients of determination (R^2) for the linear fitting equations established for each analytical spectral line were 0.997 5, 0.925 8, 0.916 1, and 0.851 0, respectively, indicating strong linear relationships between elemental content and spectral intensity. Furthermore, the average relative standard deviations (RSD) corresponding to each fitting equation were 12.43%, 21.35%, 21.02%, 16.84% and 1.82%, 4.12%, 1.00%, 2.04%, respectively, indicating controllable data dispersion and high system stability. Additionally, the relative errors (RE) of the quantitative results for each element in the two validation sets were 0.71%, 1.83%, 8.33%, and 0.35%, respectively, indicating good predictive accuracy. Overall, the comprehensive evaluation based on R^2, RSD, and RE indicators indicates that the multi-fiber collection LIBS system constructed in this study enables synchronous high-precision quantitative analysis of multiple elements (Mn, Cr, Fe), providing technical support for high-precision applications of LIBS.

Keywords laser-induced breakdown spectroscopy (LIBS); plasma; spatial distribution of elements; multi-element quantitative analysis; manganese steel

HIGHLIGHTS

1) The two-dimensional spatial distribution characterization of elements in laser-induced plasma was realized by using a multi-fiber LIBS system.
2) The inhomogeneity of element distribution and the spatial aggregation characteristics of spectral line intensity in manganese steel laser plasma were investigated.
3) The calibration curves based on the multi-fiber collection system showed high linear correlation.